# Extra high-Q resonances and extraordinary transparency in finite fragments of dielectric metasurfaces: prospects for 5G applications

**Saeid Jamilan*, Varsha Vijay Kumar, Muhammad Danyal, and Elena Semouchkina**

**AFFILIATIONS**
*Department of Electrical and Computer Engineering, Michigan Technological University, Houghton, MI, 49931, USA*
*sjamilan@mtu.edu*

**ABSTRACT:** We investigate the effects of fragmenting metasurfaces (MSs), composed of dielectric disks, on their electromagnetic responses and show that the presence of four abrupt boundaries between finite size structures and free space leads to the formation of new resonance modes. In addition to characteristic for infinite metasurfaces modes with identical dipolar resonances formed in all unit cells, fragmented metasurfaces can exhibit out-of-phase electric and magnetic responses in neighboring "meta-atoms". While in-phase responses correspond to field patterns representative for even resonance modes, out-of-phase responses produce a variety of patterns typical for odd resonance modes. These modes are formed as the result of partial reflections of surface waves from boundaries between MS fragments and free space, and their respective responses demonstrate extremely high intensities and Q-factors. Enabled by new responses significant localized wave/matter interaction can be used for enhancing the performance of sensors and absorbers of 5G systems. In addition, we report the detection of extraordinary narrow-band transmission at electric and magnetic dipolar resonances in fragmented MSs that can be used to locally enhance mm-wave signals for 5G communications. As a proof of concept, transmission through a 5×5 MS fragment has been experimentally confirmed in the X-band of microwave spectrum.

Fifth generation (5G) wireless communication systems are required to provide high-rate data transfer and robust connectivity for the drastically increasing number of mobile devices, which use data-consuming applications and services [1]. In comparison with 4G communication systems, 5G systems could utilize higher frequency bands from 24.25 GHz to 52.6 GHz. Realization of 5G systems needs advanced electromagnetic devices, such as highly directive antennas, beam steerers, lenses, filters, sensors, and absorbers for mm-wave range [2]. Meta-surfaces (MSs), being planar lightweight structures, which operate due to resonances in constituent elements, were found to present a promising platform for implementing such devices [3-10]. However, most of recently developed 5G components based on MSs include conductive elements, which, at higher frequencies, cause increased losses and additional attenuation of electromagnetic signals on shorter distances. Low-loss dielectric MSs, known to outperform even plasmonic MSs, whose designs incorporate dielectric and metallic counterparts, promise significant advantages for 5G systems.

Similar to metamaterials, MSs consist of periodically arranged unit cells and represent, in fact, single planes of metamaterials. Therefore, MS responses are conventionally analyzed by modeling single unit cells with periodic boundary conditions. This approach assumes identical responses from all unit cells. MS responses are defined by interaction between waves incident on MS plane and resonances in "meta-atoms". The resonances in dielectric MSs, i.e., in MS composed of dielectric resonators (DRs), can be typically

considered analogous to Mie resonances, with the basic types being dipolar electric and magnetic ones. Since Mie-type dipolar resonances perform as the sources of radiation, they are expected to initiate the formation of surface waves (SWs), propagating in MS plane. Interaction of SWs with DR lattices is controlled by diffraction processes, which could lead to collective responses in MSs, in particular, to the formation of lattice resonances (LRs). We have earlier reported about SWs and LRs in infinite dielectric MSs, investigated by numerical experiments using single cell models with periodic boundary conditions (PBCs) [11]. In real applications, however, MSs should be represented by fragments with finite number of meta-atoms, when abrupt boundaries between MS and free space could affect propagation and reflection of SWs, modifying MS responses.

In this work, we investigate electromagnetic responses of MSs of finite size, composed of dielectric disks. We demonstrate that in addition to conventional dipolar resonances with identical responses of unit cells, observed in infinite MSs, MS fragments can exhibit in neighboring meta-atoms out-of-phase electric and magnetic responses, which have much higher intensity and very high-Q factors. Such resonances enable significant localized wave/matter interaction necessary for enhancing the performance of sensors and absorbers of 5G systems. We also report detection of extraordinary transmission at electric and magnetic dipolar resonances in dielectric MSs that can be used to locally enhance mm-wave signals for 5G communications.

Full-wave simulations of electromagnetic responses from MSs, composed of identical dielectric disks, were performed by using COMSOL Multiphysics and CST Studio Suite software packages. Arrays of disks were arranged in free-space on xy-plane, while their heights/thicknesses were extended along z-axis. Electric (E) and magnetic (H) components of incident wave were polarized, respectively, along x- and y-axes, while z-directed wave vector was normal to MS plane. For simulating fragmented MSs, a finite set of disks was placed in the computational domain filled with free space and terminated by perfectly matching boundaries (PMBs). Such model mimicked infinite free space around MS fragments under study. For analyzing infinite MSs, we simulated single unit-cell model with PBCs applied at xz and yz boundaries of the cell [11]. The lattice constants marking the distance between centers of neighboring DRs in x- and y-directed rows were defined as $\Delta_X$ and $\Delta_Y$, respectively. They were either equal: $\Delta = \Delta_X = \Delta_Y$ (square lattices) or different (rectangular lattices). Disks were made of ceramic material with the dielectric constant of 37.2 and had the diameter and the height of, respectively, 6 and 3 mm. At such parameters, dipolar resonances in DRs were excited within the microwave X-band for the convenience of experiments. However, we show that all features of the observed characteristics of these MSs can be reproduced in MSs, which operate in 5G frequency range, being composed of resonators with properly re-scaled dimensions and made of proper material.

Fig. 1 allows for comparing 3D spectra of magnetic resonance responses for infinite MSs and 5×5 MS fragments at different lattice constants. Resonance responses are characterized by signal spectra from H-field probes placed either in centers of unit cells employed at modeling infinite MSs, or in centers of central cells of MS fragments. For magnetic dipolar resonances, which are oriented along y-direction at the described above excitation type, primary radiation is expected along x-direction that defines the choice of $\Delta_X$ as the changing lattice parameter in Fig. 1, which was varied between 7 mm and 35 mm. The lattice parameter $\Delta y$ was kept constant and equal to 7 mm. Similar 3D spectra could be obtained for electric dipolar resonance responses at the changes of $\Delta y$ lattice parameter from 7 mm up to 35 mm and fixing $\Delta_X$=7 mm.

As seen in Fig. 1a, at increasing lattice constant $\Delta_X$, magnetic response observed in infinite MS experiences red shifting (shifts to longer wavelengths) and asymptotically approaches the line marking the Rayleigh anomaly (RA), when the wavelength of incident wave becomes comparable to the lattice constant.

We discussed such red shifting of dipolar resonances in [11]. Similar effects were earlier noticed in [12] at the studies of planar arrays of spherical silicon resonators. According to [12], at lattice constants, comparable to the wavelengths of radiation, diffraction of surface waves, which are initiated by elementary electric and magnetic resonances, should lead to the formation of surface LRs, interplay of which with elementary dipolar resonances could cause their red shifting.

Fig. 1b, which presents H-field signal spectra for 5×5 MS fragment, shows that in addition to response with characteristic red shifting, MS of finite size demonstrates very strong response at $\Delta_X > 12.5$ mm, formed by coinciding branches, which are split at $\Delta_X < 12.5$ mm. New response forms an extremely narrow vertical line, indicating that its resonance frequency is fixed in a wide range of lattice constants. The Q-factor of the new narrow-band resonance appears to be much higher than Q-factor of the resonance, characteristic for infinite MSs. Another vertical line of less strength, caused by additional narrow band resonance, is seen in the longer wavelength part of the spectrum.

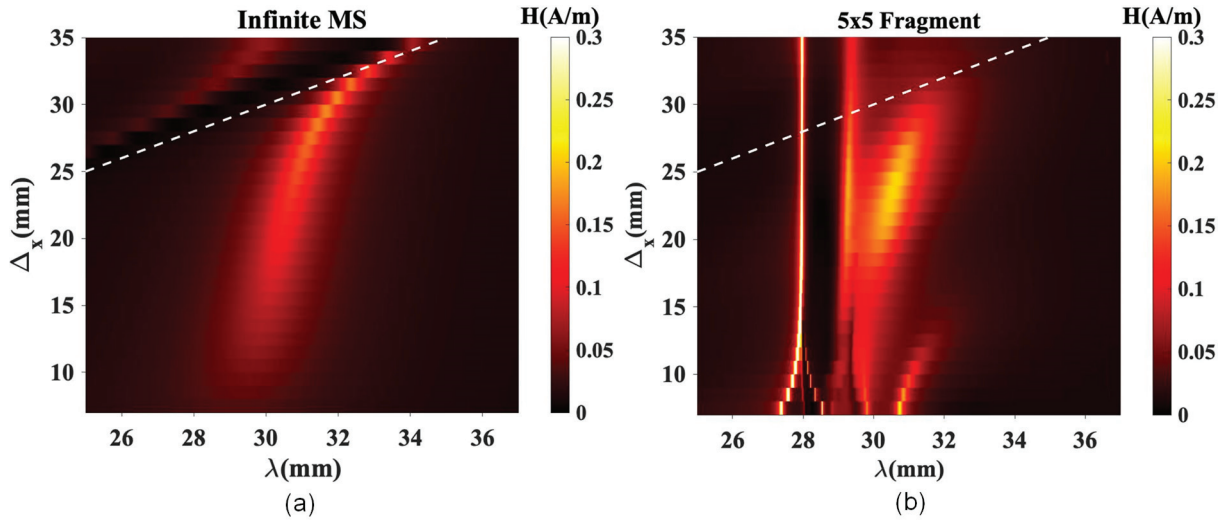


**FIG. 1.** Spectra of magnetic resonance responses at increasing the lattice constant $\Delta_X$ in the direction normal to orientation of magnetic dipoles for (a) infinite MSs and (b) 5×5 MS fragment. Lattice constant $\Delta_Y$ is kept constant and equal to 7 mm.

To characterize a variety of resonances observed in finite MSs, Fig. 2 presents the spectra of H- and E-probe signals, observed in the central DR of 5×5 fragment of MS with square lattice and lattice constant $\Delta$ = 10 mm. Fig. 2 also presents H- and E-field patterns in the median xy-cross-section of the fragment at peak frequencies of the spectra. As seen in Fig. 2a, the H-field peak at 10.214 GHz (correlated with the response experiencing red shifting in Fig. 1b) corresponds to the formation of coherent magnetic dipolar resonances in all DRs of the fragment (we can consider this case as the formation of even magnetic resonance mode). Similar coherent oscillations are observed at magnetic dipolar resonances in infinite MSs (corresponding to the response shown in Fig. 1a). Two sharp higher frequency H-field peaks in Fig. 2a (correlated with two responses with fixed resonance frequencies in Fig. 1b) and H-field peak at 9.93 GHz in Fig. 2a correspond to out-of-phase oscillations in neighboring DRs, i.e., to the formation of odd magnetic resonance modes. Odd modes apparently originate from partial reflections of SW from boundaries between fragmented MSs and free space. The strengths and high Q-factors of most prominent odd-mode resonances could be explained by mutual compensation of radiation generated by elementary dipolar resonances with opposite (shifted by $\pi$ radians) phases of oscillations.

Presented in Fig. 2b E-field signal spectrum for the same 5×5 MS fragment has the structure comparable with that of magnetic response, seen in Fig. 2a, except for the fact that even mode appears at the high frequency shoulder of the strongest peak in the spectrum. Coupled sharp peaks, seen in both E- and H-field responses, correspond to comparable arrangements of electric and magnetic dipolar resonances in neighboring DRs in MS plane. The peaks in the middle of both spectra exhibit chess board-type alteration of dipolar resonances in MS plane with opposite phases of oscillations in nearest DRs. However, while high frequency H-field peak is defined by reflections of SWs propagating in y-direction, its electric counterpart appears related to reflections of waves traveling in x-direction.

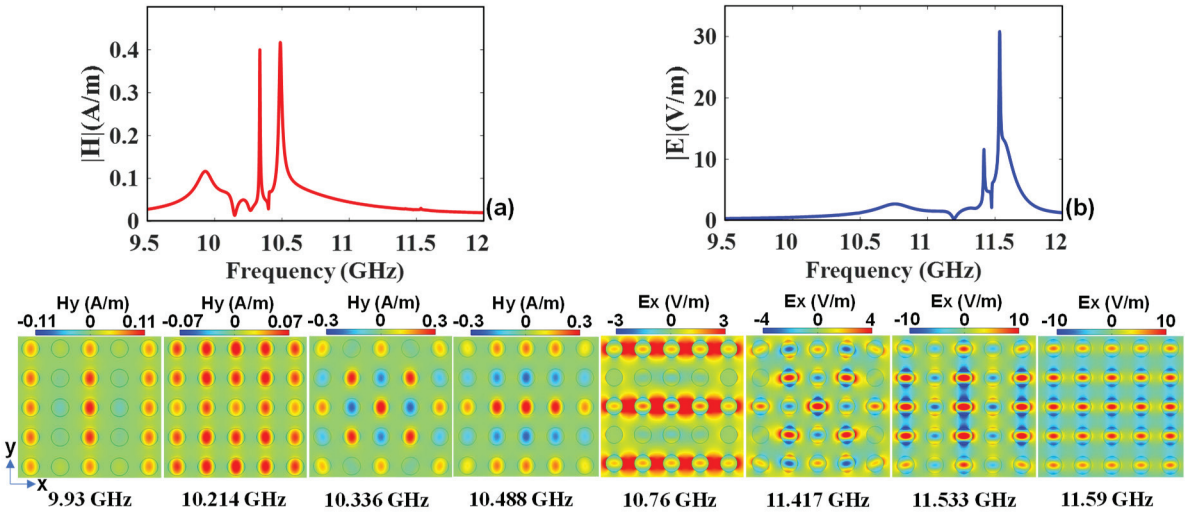


**FIG. 2.** (a) Magnetic and (b) electric responses from 5×5 MS fragment with Δ = 10 mm. Field patterns in the lower row are obtained at peak frequencies of the spectra.

To disclose the role of the boundaries between finite MSs and free space in the formation of resonance modes in fragments, we investigated responses from semi-infinite MSs, i.e., MSs with periodic boundaries (PBCs) applied at MS termination by either xz- or yz-planes, while at orthogonal planes, PMBs were terminating computational domain. Figs. 3a and 3b present magnetic and electric responses of MSs, which are infinite in y-direction and comprise only 3 cells in x-direction. The simulation model was composed of 3×3 cells with non-periodic boundaries at MS termination by yz-planes and PBCs at xz boundaries of MS termination. Figs. 3c and 3d present the responses for alternative case, i.e., for MS, infinite in x-direction and comprising 3 cells in y-direction, represented by the model comprised of 3×3 unit cells with PBCs at yz-boundaries and non-periodic boundaries at xz-planes. In difference from finite MS fragments, characterized in Figs. 1 and 2, semi-infinite MSs supported only two modes, one of even type, similar to that observed in infinite MSs and another one of odd type, formed due to SW reflections from boundaries between MS fragment and free space. No field patterns with chess-board type arrangement of dipoles could be observed in semi-infinite MSs, since reflections can be provided only for SWs traveling in either x- or y-direction, but not in both. It can be noticed in Fig. 3 that, while spectral positions of even electric and magnetic modes do not depend on whether MS is infinite in y- or in x-direction, the positions of odd modes in the spectra are changing significantly at changes of MS geometry. This can be explained by the fact that odd modes in MSs, infinite in y-direction, have identical phases of resonance oscillations in DRs located in

columns, while in MSs, infinite in x-direction, identical phases of resonance oscillations are observed in rows of DRs. This makes configurations of field distributions for two odd modes quite different.

The specifics of field patterns presented in Fig. 3 allows for relating the observed modes to even and odd transmission modes, known in photonic crystals (PhCs). Although dipolar resonances are excited in constituent "atoms" of MS by normally incident wave, the presence of SWs, propagating in MS plane, apparently leads to the formation of MS responses, which are similar to responses of PhCs. In MSs, infinite in both directions, PBCs, at plane wave incidence, allow for the formation of only coherent resonances in DRs. The presence of non-periodic boundaries in MSs, providing for multiple reflections of SWs, could make MSs performing similar to PhCs, even with only 3 unit cells between non-periodic boundaries (Fig. 3).

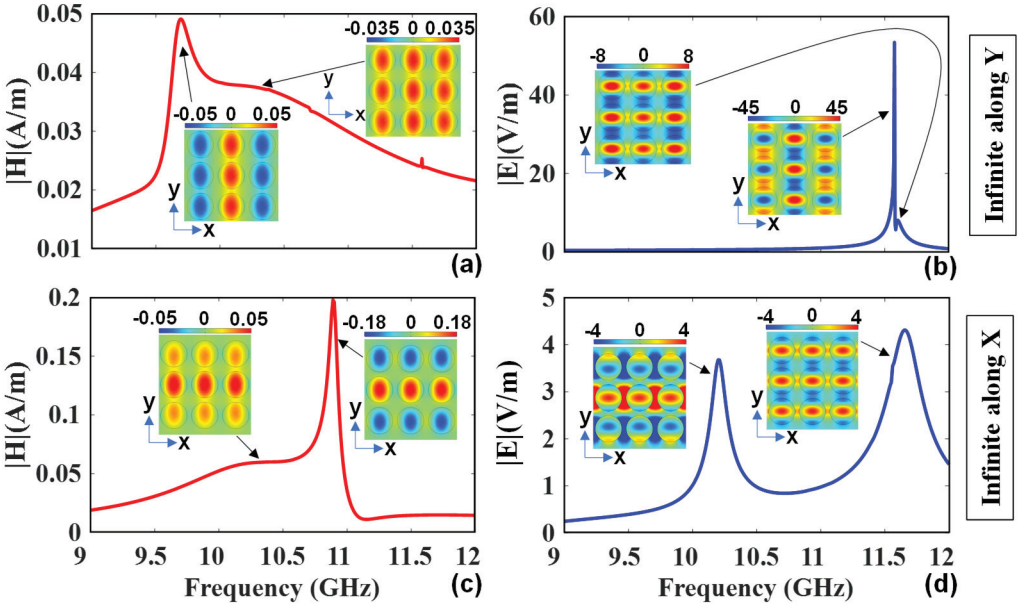


**FIG. 3.** Magnetic (a, c) and electric (b, d) responses from central DR of 3×3 sections of semi-infinite MSs with lattice constant with Δ = 7 mm, having: (a, b) PBC at xz boundaries and non-periodic conditions at yz-boundaries and (c, d) PBC at yz-boundaries and non-periodic conditions at xz-boundaries. Field patterns of Hy-field (two on the left) and of Ex-field (two on the right) in xy cross-sections of 3×3 sections of respective semi-infinite MSs at frequencies of main spectral peaks.

One more observation from Fig. 3 is that E-field intensities in the resonance spectra presented for MS fragments with non-periodic yz-boundary (Fig. 3b) are significantly stronger than E-field intensities in the spectra of MS fragments with non-periodic xz-boundary (Fig. 3d). The Q-factor of odd mode resonance is also much higher in the former case. This could be explained by the fact that non-periodic boundaries of MSs, while providing for multiple partial reflections of SWs, allow energy to flow away, thus decreasing the strength of resonances. The revealed difference between Figs. 3b and 3d is in correspondence with mentioned above specifics of radiation from dipolar resonances: at electric response, radiation occurs primarily in the direction normal to the orientation of electric dipoles, i.e., along y-axis, while at magnetic response, radiation is expected primarily in the direction normal to the orientation of magnetic dipoles, i.e., along x-axis. As the result, non-periodic yz- boundaries at electric response should not affect the formation of electric resonances (Fig. 3b), while non-periodic xz-boundaries at electric response should provide leakage of resonance energy from MS, decreasing the resonance strengths (Fig. 3d). At magnetic response,

non-periodic yz-boundaries should provide leakage of resonance energy, decreasing the resonance strengths (Fig. 3a), while non-periodic xz-boundaries should not affect the formation of magnetic resonances (Fig. 3c).

Another effect, important for practical application of MSs, is extraordinary transmission, which can be detected in dielectric MSs at dipolar resonances. At the studies of electric responses from dense infinite dielectric MSs, irradiated by normally incident plane waves, we have revealed the phenomenon, analogous to the known in atomic physics electromagnetically induced transparency (EIT) [13]. The main specific of the new phenomenon was an occurrence of a narrow transparency window at the frequencies of electric dipolar resonances in disk-shaped DRs, when total reflection, instead of transmission, was generally expected. Investigation of Fano resonances, accompanying the new effect, allowed for relating it to destructive interference of background radiation and radiation produced by oscillations of resonance fields in MS "atoms". Magnetic resonances in dense infinite MSs were very weak and could not produce similar effects. However, as it is seen from the presented above data, fragmented MSs demonstrate significant enhancement of the strength of magnetic resonances, so that accompanying unusual transparency can be expected.

For infinite MSs, modeled by using single unit cells with PBCs, transmission spectra (T) at plane wave incidence can be obtained using simulated scattering parameters T = |S21|. In the case of finite MS fragments, transmission spectra can be found based on the approach proposed in [14] by using the relation: $T = \frac{FS}{FS+BS}$, where FS is the power (W/m$^2$) scattered by the fragment in forward direction (+z) and BS – power scattered by the fragment in backward direction, with respect to the direction of incident wave flow (-z). Fig. 4 presents transmission spectra for two MS fragments with different quantity of DRs in comparison with S21 spectrum calculated for infinite MS. All MSs have dense square lattices with lattice constant $\Delta$ = 7 mm. As seen in the figure, all obtained spectra coincide at frequencies f < 10 GHz, where MS responses experience Kerker's effect [15], and in the vicinity of electric dipolar resonance at about 11.6 GHz, where EIT is observed. It should be noticed, however, that transmission peaks at the electric resonance have higher Q-factors for MS fragments, in comparison with the peak obtained for infinite MS. As expected, S21 spectrum of infinite MS does not demonstrate any peaks in the vicinity of magnetic resonance, since dense infinite MSs support only very weak magnetic resonances [13].

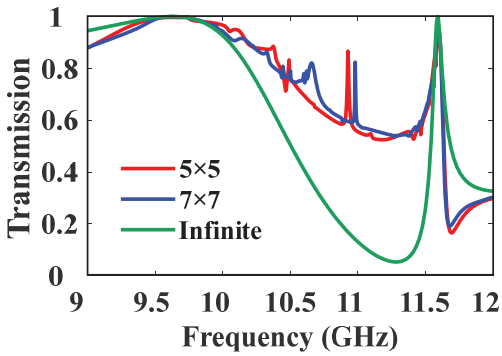


**FIG. 4.** Transmission spectra for 5×5 and 7×7 MS fragments in comparison with |S21| spectrum of infinite MS. All MSs have square lattice with $\Delta$ = 7 mm.

In difference from the spectrum of infinite MS, transmission spectra of finite MS fragments exhibit additional sharp peaks, with spectral positions corresponding to the magnetic dipolar resonance in DRs.

These peaks are almost coinciding for two MS fragments; however, they appear on the background of high transmission. Since in finite MSs with square lattices leakage of the resonance energy could occur at all four boundaries of MS fragments, this could decrease the contrast of resonance effects.

To mitigate the above problem, we investigated transmission spectra of fragments with small $\Delta_Y$, but extended $\Delta_X$, i.e., fragments with the geometry approaching that of MS, semi-infinite in x-direction, for which stronger odd magnetic resonance mode was observed (Fig. 3c). Fig. 5a presents transmission spectra for MS fragments with $\Delta_Y = 7$ mm and $\Delta_X$ increasing from 10 mm to 25 mm. As seen in the figure, increasing $\Delta_X$ leads to the formation of a very sharp and strongly pronounced transmission peak at expected frequency of dipolar magnetic resonance of about 10.7 GHz. The peak transparency is approaching 0.83. Although it does not achieve 1 and, so, does not confirm full transparency, as in the case of electric resonance, it demonstrates much higher Q-factors (400, 1087, and 1482 at, respectively, $\Delta_X = 10$, 15, 25 mm) that is characteristic for EIT. Field patterns, obtained in xy-cross-sections of MS fragments at $f = 10.7$ GHz demonstrated the formation of odd magnetic resonance modes. Additional investigations are required to ensure that the observed peak of MS transparency is defined by the phenomenon of EIT-type.

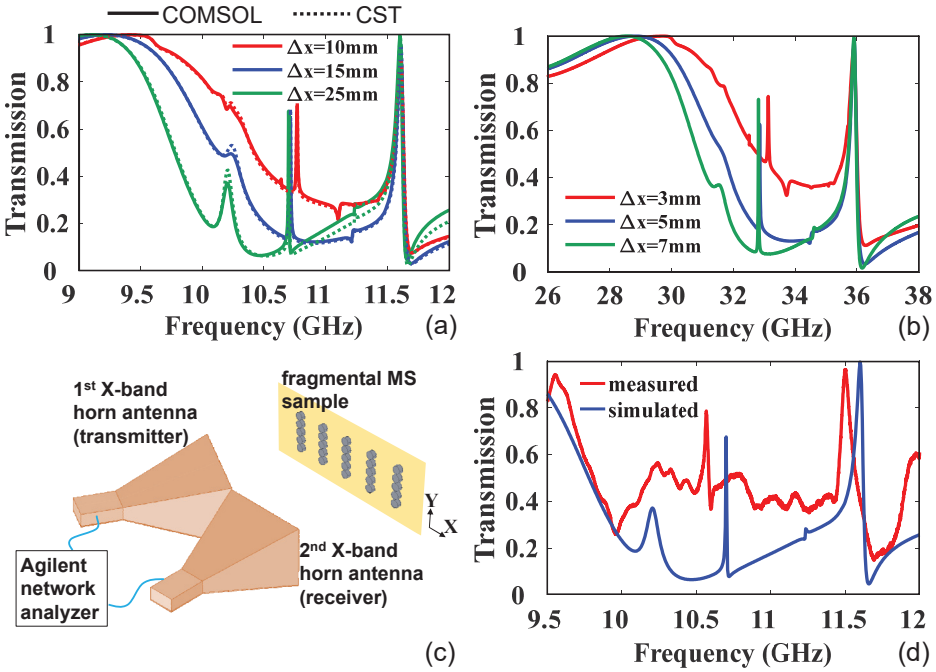


**FIG. 5.** (a) Simulated transmission spectra (solid curves-COMSOL, dashed curves-CST) for 5×5 MS fragments, operating in X-band, with lattice constants: $\Delta_Y = 7$ mm and $\Delta_X$: 10 mm, 15 mm, and 25 mm. (b) Simulated transmission spectra for 5×5 MS fragments, operating in 5G range, with lattice constants: $\Delta_Y = 2.5$ mm and $\Delta_X$: 3 mm, 5 mm, and 7 mm. (c) Schematics of experimental setup for measuring reflections. (d) Measured and simulated transmission spectra for X-band 5×5 MS fragment with $\Delta_Y = 7$ mm and $\Delta_X = 25$ mm.

Fig. 5a was obtained by using two different computational solvers (COMSOL and CST) to verify our simulation results. Fig. 5b demonstrates that similar effects of extraordinary transparency can be reproduced in MSs, which operate in 5G frequency range. MSs were composed of disks made of lossless ceramic material (Barium Zinc Cobalt Niobate [16]), having relative permittivity of 35. The diameter and height of the disks were equal to 2 mm and 1 mm, respectively. These results are promising for employing magnetic

and electric resonances in finite dielectric MSs for 5G applications. Furthermore, we experimentally measured transmission spectrum for 5×5 fragment with $\Delta_Y$ = 7 mm and $\Delta_X$ = 25 mm. We used two X-band horn antennas and an Agilent vector network analyzer to measure the reflections (R) from the fragment as shown in the schematics of Fig. 5c. Then, we calculated the measured transmission (T) as T=1-R. Fragmented MS sample was made by arranging ceramic disks on a thin and firm paper board by double-stick tapes. Fig. 5d demonstrates that measured and simulated transmission spectra are in a reasonable agreement and expected peaks of MS transparency are clearly detected.

Table I presents Q-factors and amplitudes of electric and magnetic resonances for single DR and different MS geometries considered above. In all simulations, for illuminating the structures, we used identical incident plane waves with amplitude of 1 V/m for E-field and $1/120\pi$ = 0.0026 A/m for H-field. As seen from the Table, odd-mode resonances in MS fragments provide much higher amplitudes and Q-factors in comparison with resonances in single DRs and infinite MS (with similar periodicity). Increasing the number of resonators in finite MSs leads to higher Q-factors and amplitudes of electric and magnetic responses. With such extraordinary characteristics demonstrated in Table I, fragments of dielectric MSs can be considered as a promising host for realizing very significant wave/matter interactions, which are requested in numerous applications such as absorbing and sensing devices [17-20].

**TABLE I.** Q-factors and amplitudes of magnetic and electric resonances for various cases.

| | Magnetic resonance | | | Electric resonance | | |
|---|---|---|---|---|---|---|
| Case | Q-factor | Amplitude (A/m) | Mode | Q-factor | Amplitude (V/m) | Mode |
| Single disk | 20 | 0.16 | even | 26 | 8 | even |
| Infinite MS (Δ=7mm) | 4 | 0.03 | even | 94 | 10 | even |
| 3×3 fragment (Δ=7mm) | 120 | 0.29 | odd | 1,060 | 33 | odd |
| 5×5 fragment (Δ=7mm) | 448 | 0.54 | odd | 6,808 | 75 | odd |
| 7×7 fragment (Δ=7mm) | 1,100 | 0.73 | odd | 16,500 | 115 | odd |

## ACKNOWLEDGEMENT

The authors would like to thank Dr. G. Semouchkin for many useful discussions. This work was supported by the National Science Foundation (NSF) under Award No. ECCS-1709991.

## DATA AVAILABILITY

The data that support the findings of this study are available from the corresponding author upon reasonable request.

## REFERENCES

1. H. Hao, D. Hui, and D. Lau, "Material advancement in technological development for the 5G wireless communications," Nanotechnology Reviews, 9 (1), 683-699, 2020.
2. R. Waterhouse and D. Novack, "Realizing 5G: Microwave Photonics for 5G Mobile Wireless Systems," IEEE Microwave Magazine, 16 (8), 84-92, 2015.
3. A. A. Brazález, L. Manholm, M. Johansson, M. Mattsson and O. Quevedo-Teruel, "A Ka-band glide-symmetric planar Luneburg lens with combined dielectric/metasurface for 5G communications," 2018 International Symposium on Antennas and Propagation (ISAP), Busan, Korea (South), 2018.
4. N. Hussain, M. Jeong, A. Abbas, T. Kim and N. Kim, "A metasurface-based low-profile wideband circularly polarized patch antenna for 5G millimeter-wave systems," IEEE Access, 8, 22127-22135, 2020.
5. C. Xue, Q. Lou and Z. N. Chen, "Broadband double-layered huygens' metasurface lens antenna for 5G millimeter-wave systems," IEEE Transactions on Antennas and Propagation, 68 (3), 1468-1476, 2020.
6. Z. Li, Y. Mu, J. Han, X. Gao, and L. Li, "Dual-polarized antenna design integrated with metasurface and partially reflective surface for 5G communication," EPJ Appl. Metamat., 7, 2020.
7. D. Rotshild, E. Rahamim, A. Abramovich, "Innovative reconfigurable metasurface 2-D beam-steerable reflector for 5G wireless communication," Electronics, 9, 1191, 2020.
8. Z. N. Chen, T. Li and W. E. I. Liu, "Microwave metasurface-based lens antennas for 5G and beyond," 2020 14th European Conference on Antennas and Propagation (EuCAP), Copenhagen, Denmark, 2020.
9. H. Votsi, A. Bilal, K. Neophytou, A. Kanno, T. Kawanishi, M. Antoniades, and S. Iezekiel, "Photonically enabled metasurfaces for 5G," 2020 XXXIIIrd General Assembly and Scientific Symposium of the International Union of Radio Science, Rome, Italy, 2020.
10. T. Ramachandran, M. R. I. Faruque, A. M. Siddiky, and M. T. Islam, "Reduction of 5G cellular network radiation in wireless mobile phone using an asymmetric square shaped passive metamaterial design," Scientific Reports, 11, 2619, 2021.
11. S. Jamilan and E. Semouchkina, "Lattice resonances in metasurfaces composed of silicon nano-cylinders," 14th Intern. Congress on Artificial Materials for Novel Wave Phenomena – Metamaterials, N.Y., USA, 2020.
12. V. E. Babicheva and A. B. Evlyukhin, "Resonant lattice Kerker effect in metasurfaces with electric and magnetic optical responses," Laser & Photonics Reviews, 11, 1700132, 2017.
13. S. Jamilan, G. Semouchkin, and E. Semouchkina, "Analog of electromagnetically induced transparency in metasurfaces composed of identical dielectric disks," Journal of Applied Physics, 129, 063101, 2021.
14. T. Matsui and H. Iizuka, "Effect of finite number of nanoblocks in metasurface lens design from bloch-mode perspective and its experimental verification," ACS Photonics, 7 (12), 3448-3455, 2020.
15. S. Jamilan, G. Semouchkin, N. P. Gandji, and E. Semouchkina, "Specifics of scattering and radiation from sparse and dense dielectric meta-surfaces," Journal of Applied Physics, 125, 163106, 2019.
16. M. D. Hill and D. B. Cruickshank, "Ceramic materials for 5G wireless communication systems," American Ceramic Society Bulletin, 98 (6), 2019.
17. J. Tian, H. Luo, Q. Li, X. Pei, K. Du, and M. Qiu, "Near-infrared super-absorbing all-dielectric metasurface based on single-layer germanium nanostructures," Laser & Photonics Reviews, 12, 1800076, 2018.
18. C. F. Kenworthy, L. P. Stoevelaar, A. J. Alexander, and G. Gerini1, "Using the near field optical trapping effect of a dielectric metasurface to improve SERS enhancement for virus detection," Scientific Report, 11, 6873, 2021.

19. J. Li, Z. Chen, H. Yang, Z. Yi, X. Chen, W. Yao, T. Duan, P. Wu, G. Li, and Y. Yi, "Tunable broadband solar energy absorber based on monolayer transition metal dichalcogenides materials using Au nanocubes," Nanomaterials, 10(2), 257, 2020.
20. Y. Wang, Z. Chen, D. Xu, Z. Yi, X. Chen, J. Chen, Y. Tang, P. Wu, G. Li, and Y. Yi, "Triple-band perfect metamaterial absorber with good operating angle polarization tolerance based on split ring arrays," Results in Physics, 16, 102951, 2020.